

Soft X-Ray Sensing by Gold Ion (Au⁻) Implanted Poly Methyl Methacrylate

Savita Devi¹, Kulvinder Singh²

¹(Department of Applied Physics, Singhania University, District Jhunjhunu, Pachheri Bari, Rajasthan, India.

²(Department of Physics, Deen Dayal Upadhyaya College, University of Delhi, India)

Abstract: Multiple applications of X-rays in material science are imposing rising demand for effective and more user-friendly X-ray sensors. Commonly used solid-state sensors are rigid crystalline material having flat geometry. With increasing application demand for flexible and easy to shape sensor is developing fast. Keeping the demand in mind polymer-based X-ray sensors are developed with gold ion implantation. Gold ions accelerated at 80 KeV were implanted. Implanted polymer (methyl methacrylate, PMMA) sheets were subjected to Soft X-rays switching studies at room temperature. Nickel filtered X-rays from Cu target in the energy range 8.051KeV were used in the experimentation work. Studies revealed that gold ion implanted PMMA sheets show stable detection of X-rays at room temperature. Mobility-Life time product was obtained using the iterative method. It ranges in the order of $10^{-2} \text{cm}^2 \text{V}^{-1}$. These sheets show quite low thermally generated charges at room temperature and high photocurrent. X-ray switching studies conducted on these sheets show low rise and fall time making the material good for imaging applications.

Key Word: Atomic gold ion implantation, Detectors, Polymethylmethacrylate, Sensors, X-rays.

Date of Submission: 28-10-2020

Date of Acceptance: 09-11-2020

I. Introduction

Soft X-rays of few angstrom wavelengths are commonly used as invading radiations for material analysis. There are several applications of X-rays in material science like X-ray diffraction in crystallography, X-ray energy dispersive techniques for chemical analysis, nanostructure analysis, X-ray fluorescence spectroscopy, etc. [1-13]. Set-up for these applications requires an X-ray source, material holder, and a powerful X-ray sensor. X-ray sensor is an important component of such a set-up. The most commonly used sensors are flat planer sensors. Nowadays the use of a room temperature solid-state sensor is becoming popular due to their mechanical strength and stability. [14-15]. The choice of sensor material is based on the number of criteria like photo conversion into mobile charges, mobility-life time products of carriers, stability with time and variation of external conditions, etc. [14]. In the number of applications, flexible sensors are of additional benefit. For example, in taking the oscillating crystal diffractogram, a cylindrical-shaped sensor plate is required. The problem with the flat sensor is the mechanical movement required to scan the diffracted X-rays in a cylindrical mechanical manner. The additional mechanical movement adds to the complexity of the set-up. While a cylindrical sensor plate will do the job without any mechanical movement.

Polymer materials are easy to process and have mechanical flexibility to shape as per requirement. As X-ray sensors, they have limited efficiency for photo conversions as major constituent atomic have a low atomic number (the atomic number for C=6, H=1.O=8). Implanted with atoms of high atomic number is one of the solutions. Keeping this in mind the present work is planned. The polymer used is Poly methyl methacrylate (PMMA) and the heavy atom selected is gold ($z=47$).

II. Material and Methods

High purity transparent clear Poly methyl methacrylate [PMMA or $(\text{C}_5\text{O}_2\text{H}_8)_n$; make DELITE] plates were used as the base material. Samples were prepared from the sheets with dimensions $1.2 \times 1.2 \times 0.3 \text{cm}^3$. Surfaces were cleaned using pure ethanol with a soft paper tissue. Samples were mounted in a vacuum chamber (pressure less than 10^{-6} torr). Gold ions (single negative charge state) were bombarded on the sample with fluence ranging from $1 \times 10^{16} / \text{cm}^2$ to $10.0 \times 10^{16} / \text{cm}^2$. The accelerating voltage was kept 80KV and the current was kept $5 \mu\text{A}$. The Beam area was kept $1 \times 1 \text{cm}^2$. Samples show slight etching on the surface and sample coloration changes from slight brownish to dark brownish. Samples were then subjected to X-ray switching studies using X-rays at 30KV from a copper target X ray tube (Philips Holland). Continuous X-rays were obtained and the beam was chopped at regular intervals. It is done by using a switching rotor device using a stepper motor. Blocking of X-rays was done with a thick semicircular lead ring. Rotation speed was controlled by a microprocessor P89C51RD2. The photocurrent was recorded by Keithley 6485 picometer. (Fig.1).

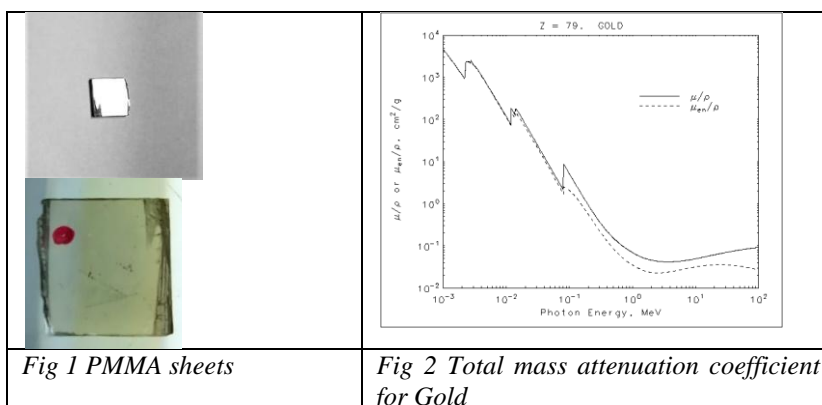


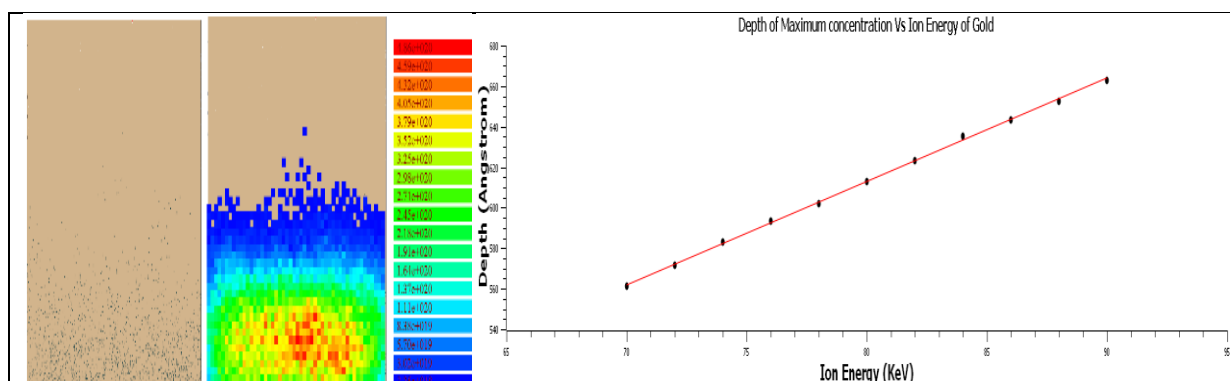
Fig 1 PMMA sheets

Fig 2 Total mass attenuation coefficient for Gold

III. Results and Discussion

Photoelectric and total mass attenuation coefficients for gold were obtained 181.48 and 184.66 cm²/g respectively corresponding to X-ray photon energy 1.54 Å (8.05 KeV) using NIST XCOM software. (Fig, 2). The contribution of coherent and noncoherent scattering is quite small in comparison to photoelectric attenuation near the 8KeV energy range. This ensures the charge pair generation during X-ray exposure. Primarily, x-ray absorption in this material is due to the photoelectric phenomenon. Elastic and inelastic scattering are comparably small. As energy is small, pair production phenomena are not expected. X-ray absorption is dominated by photoelectric absorption. It is a positive property for an X-ray detector. This ensures high electron-hole pair production. For a good detector, both quantum efficiency and spectral efficiency are to be high [16]. It is very important that charge generated, are to be collected with minimum loss to have high quantum efficiency.

Further using a 2D implant from Axcelis.com (Monte Carlo program), depth profiling of Gold implant was carried out. The results are shown in Figure. 3, for the fluence used in experimental work i.e. from 1.25X10¹⁵/cm² -14.0X10¹⁵/cm² in six steps. It was revealed that the majority of Gold ions were implanted within 70-90 Angstrom depths in the PMMA sheets for energy ranging from 640KeV to 800KeV. Moreover, with increasing fluence, the collection of Gold ions are towards the surface. This large collection of Gold near the surface causes surface etching. A similar etching is also observed in Ar/O₂ plasma. [17]. This is primarily due to chain scission done by high energy ions [18].



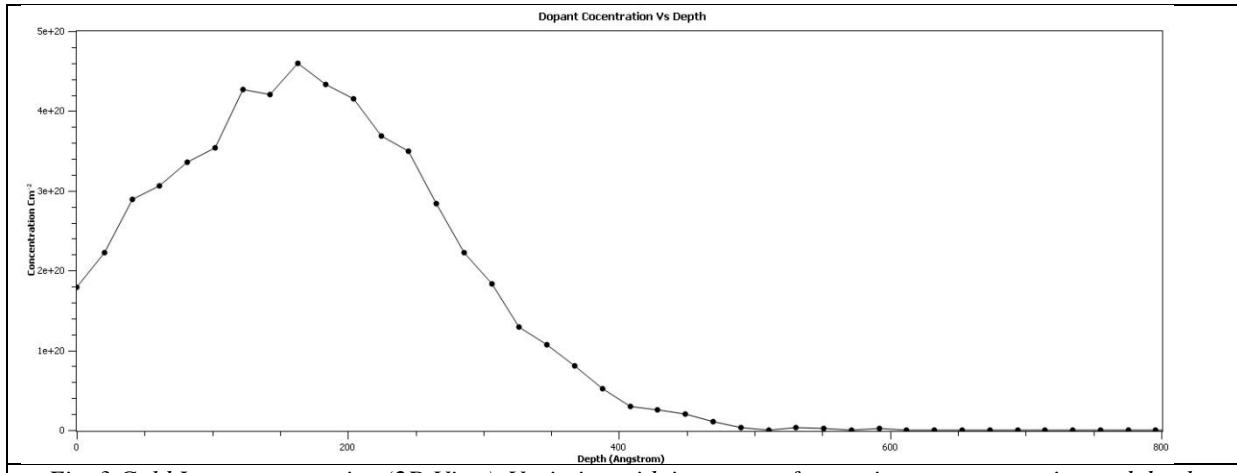
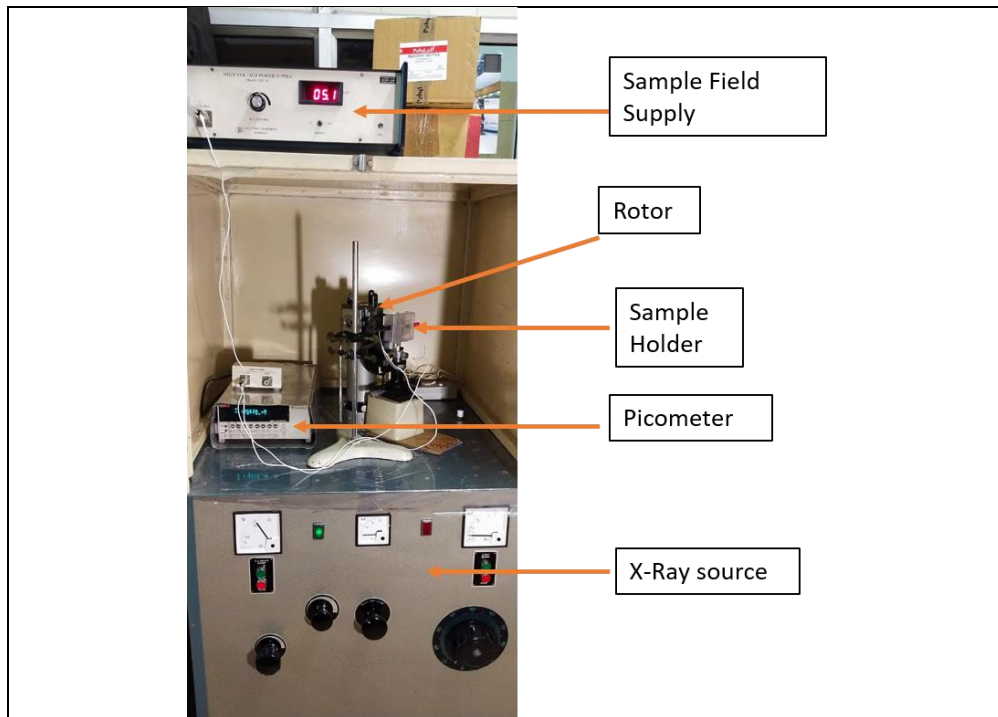


Fig. 3 Gold Ions concentration (2D View), Variation with ion energy for maximum concentration and depth Profile.

One of the most important parameters of X-ray sensor material is its mobility lifetime product. This parameter was calculated by using the modified Hecht equation [14 and 19].

$$Q = Q_0 \left(\frac{\mu \tau E}{d} \right) \left[1 - e^{-\left(\frac{d}{\mu \tau E} \right)} \right] + kE \dots\dots\dots(1)$$

Here Q represents charge collection by photo generation, μ is the mobility of charge carriers, τ is lifetime, E is the electric field, d is the thickness of the sample, k is the correction coefficient. The term kE is added for the charge collection by the base material for sample holding. The value of correction coefficient 'k' will depend on the intensity of the radiation reaching the base material and charge generation by the medium due to highly ionizing radiation. The charge collection is directly proportional to the photocurrent generated. To obtain the photocurrent gold implanted PMMA sheets were subjected to the switching studies. (Fig 4).



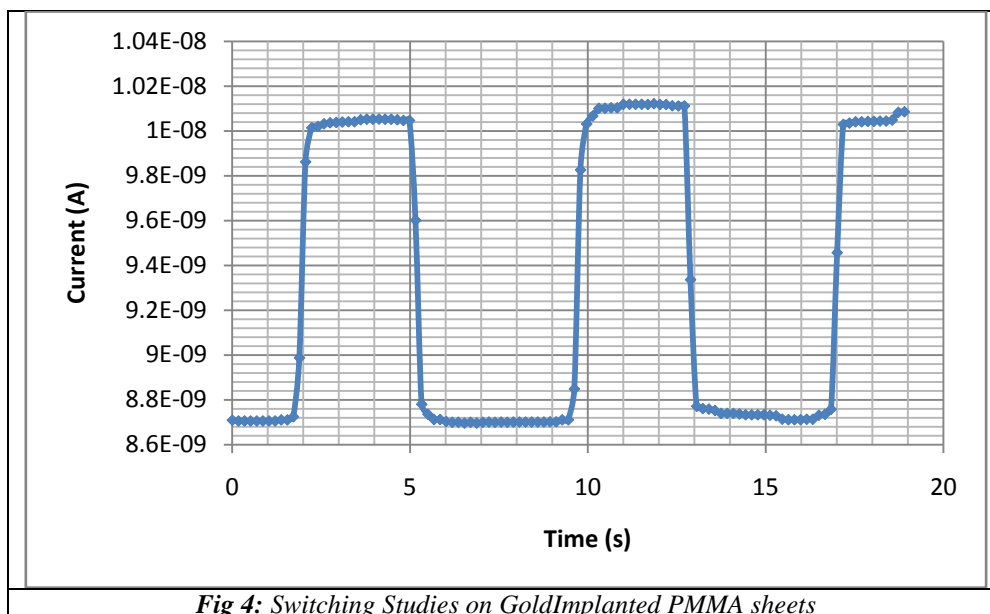


Fig 4: Switching Studies on Gold Implanted PMMA sheets

The X-ray beam is obtained from the Cu target tube operating at 30 kV at 30 mA and passing through the Nickel filter giving K_{α} line. The Beam line is chopped off at regular intervals and allowed to pass through the gold implanted PMMA sheets. Two gold electrodes are made at spacing 3.2 mm. A beam falls on the sheet perpendicular to its plane and electric field. The current through the sample is recorded by a picometer. The switching curve (Fig. 4) is obtained. Current through the sample at the time of X-Ray falling on the sample is I_{Max} and in its absence is I_{Min} . Photocurrent $I_{Ph} = I_{Max} - I_{Min}$ (2)
Equation 1 in the form:

$$I_{Ph} = I_{Ph}|_0 \left(\frac{\mu\tau E}{d} \right) \left[1 - e^{-\left(\frac{d}{\mu\tau E} \right)} \right] + k' E \dots\dots\dots(3)$$

Here $K' = k/t$.

In this method, large numbers of iterations were done by changing values of $\mu\tau$ and k' , up to the values where the normalized error became minimum and stable. The experimental results were approached to theoretical results. Experimental graphs were compared with theoretical graphs obtained by the iterative method and were found to be nearly the same.

In our case, it is a PMMA sheet. Although PMMA has very high resistivity, yet a small contribution is made by the base material. The correction coefficient “k” will depend on the intensity of the radiation reaching the base material as well as charge generation by the medium due to highly ionizing radiation. Using the iterative method mobility-life time product was found to be $2.0-8.3 \times 10^{-3} \text{ cm}^2 \text{V}^{-1}$. The value is sufficiently high for a good detector material.

IV. Conclusion

Soft X-ray detection studies conducted on Gold implanted PMMA revealed that it is a promising material. PMMA sheets can be cast in any shape. It is the most advantageous characteristic of this material. However, controlling etching during implantation is a challenge.

Acknowledgment

Author² would like to thank Inter-University Accelerator Centre, Delhi for providing facilities for Gold Implantation (Project No.61519) and L’ Orgueil Physics Centre, Delhi for providing X-ray switching studies. The author is also thankful to Axcelis.com for providing a complimentary copy of 2D Implant Simulator software.

References

- [1]. S. Bates; G. D. Zografi; D.Engers; K.Morris, Analysis of Amorphous and Nanocrystalline solids from Their X-Ray Diffraction Pattern, 2006 Pharmaceutical Research 23(10) 2333-49
- [2]. R. Das; M. E. Ali; S. B. A. Hamid. Current Applications of X-Ray Powder Diffraction-A Review. Rev.Adv.Mater. Sci. 38 (2014) 95-109

- [3]. S. Atipamula; V. R. Vangala -X-Ray crystallography and its Role in Understanding the Physicochemical Properties of Pharmaceutical Cocrystals -Journal of Indian Institute of Science 97.227-243 (2017)
- [4]. S.R/Byrn; G. Zograf; X. Chen -X-Ray Crystallography and Crystal Packing Analysis DOI.org/10.1002/9781119264408 (2017)
- [5]. Aaltonen, J.; Alleso, M.; Mirza, S.; Koradia, V.; Gordon, K. C.; Rantanen, J. Solid Form Screening—A Review. Eur. J. Pharm. Biopharm. 2009, 71, 23–37
- [6]. Benmore, C. J.; Soignard, E.; Amin S. A. Structural and Topological Changes in Silica Glass at Pressure. Phys. Rev. B 2010, 81, Article ID 054105
- [7]. Cardell, C.; Guerra, I.; Romero-Pastor, J.; Cutrone, G.; RodríguezNavarro, A. Innovative Analytical Methodology Combining Micro-X-ray Diffraction, Scanning Electron Microscope-Based Mineral Maps, and Diffuse Reflectance Infrared Fourier Transform Spectroscopy to Characterize Archeological Artifacts. Anal. Chem. 2009, 81, 604–611.
- [8]. A. KvikX-ray Diffraction, Material Science Applications. 2016 DOI 10.1016/B978-0-12-803224-4.00198-9
- [9]. Causin, V.; Marega, C.; Marigo, A.; Ripani, L. Forensic Differentiation of Paper by X-ray Diffraction and Infrared Spectroscopy. Forensic Sci. Int. 2010, 197, 70–74
- [10]. Eckardt, R.; Krupicka, E.; Hofmeister, W. Validation of Powder X-ray Diffraction Following EN ISO/IEC 17025. J. Forensic Sci. 2012, 57, 722–737.
- [11]. Eunice, E. U.; Blessing, D. C.; Fabian, O. XRD Characterization of Sand Deposit in River Niger (South-Eastern Nigeria). Am. Chem. Sci. J. 2013, 3(3), 287–293.
- [12]. Kishi, A. Detailed Observations of Dynamic Changes Such as Phase Transitions, Melting, and Crystallization Using an XRD-DSC with a High-Speed, High-Sensitivity Two-Dimensional PILATUS detector. Rigaku J. 2011, 27, 9–14.
- [13]. R. Ballabriga, I. J. Alozy, M. Campbell, E. Frojdh, E.H.M. Heijne, T. Koenig, X. Llopart, J. Marchal, D. Pennicard, T. Poikela, L. Tlustos, P. Valerio, W. Wonga, and M. Zuber, Review of hybrid pixel detector readout ASICs for spectroscopic X-ray imaging, Journal of Instrumentation, 2016 JINST 11 P01007
- [14]. Kulvinder Singh, X-Ray Switching Studies on Mercury-Poly-Methyl-Methacrylate Composites, Indian Journal of Applied Research IJAR Oct-2016 Page 161-163, Vol6, Issue-10
- [15]. Gaurav Suryan Kulvinder Singh, X Ray Switching Studies Of Bismuth(III) Oxide And Its Composites, Indian J.Sci.Res. 16 (1): 93-97, 2017
- [16]. Peter Trueb, Pietro Zambon, and Christian Broennimann, Assessment of the spectral performance of hybrid photon counting x-ray detectors, Medical physics, 44(9), 2017
- [17]. Changchun Zhang, Chunsheng Yang and Duifu Ding, Deep Reactive Ion Etching of commercial PMMA in O₂/CHF₃, and O₂/Ar-based discharges, Journal of Micromechanics and Microengineering, 2004, volume 14, number 5
- [18]. J. A. Moore and Jin O. Choi ,Degradation of Poly(methyl methacrylate), Radiation Effects on Polymers, Chapter 11, pp 156–192, Chapter DOI: 10.1021/bk-1991-0475.ch011,ACS Symposium Series, Vol. 475, ISBN13: 9780841221659eISBN : 9780841213319, November 12, 1991
- [19]. Ariño-Estrada, G., Chmeissani, M., De Lorenzo, G., Kolstein, M., Puigdengoles, C., García, J. and Cabruja, E., (2014). Measurement of mobility and lifetime of electrons and holes in a Schottky CdTe diode. Journal of Instrumentation, 9(12), p.C12032.

Savita Devi, et. al. “Soft X-Ray Sensing by Gold Ion (Au-) Implanted Poly Methyl Methacrylate.” *IOSR Journal of Applied Physics (IOSR-JAP)*, 12(6), 2020, pp. 30-34.